Heat Mass Transfer (2008) 44:1485–1495
DOI 10.1007/s00231-008-0395-3

ORIGINAL

Conjugate mixed convection with surface radiation from a vertical electronic board with multiple discrete heat sources

S. M. Sawant · C. Gururaja Rao

Received: 1 September 2007 / Accepted: 28 March 2008 / Published online: 9 April 2008

Abstract The problem of combined conduction-mixed convection-surface radiation from a vertical electronic board provided with three identical flush-mounted discrete heat sources is solved numerically. The cooling medium is air that is considered to be radiatively transparent. The governing equations for fluid flow and heat transfer are converted from primitive variable form to stream function-vorticity formulation. The equations, thus obtained, are normalised and then are converted into algebraic form using a finite volume based finite difference method. The resulting algebraic equations are then solved using Gauss–Seidel iterative method. An optimum grid system comprising 151 grids along the board and 111 grids across the board is chosen. The effects of various parameters, such as modified Richardson number, surface emissivity and thermal conductivity on temperature distribution along the board, maximum board temperature and relative contributions of mixed convection and radiation to heat dissipation are studied in detail. Further, the contributions of free and forced convection components of mixed convection to board temperature distribution and peak board temperature are brought out. The exclusive roles played by surface radiation and buoyancy in the present problem are clearly elucidated.

List of symbols

A_{r1}, A_{r2}	geometric ratios, L/t and L/L_h, respectively
g	acceleration due to gravity (9.81 m/s^2)
Gr_L^*	modified Grashof number, $g\beta\Delta T_{ref}L^3/\nu_f^2$
k_s	thermal conductivity of the board material and heat source (W/m K)
k_f	thermal conductivity of air (W/m K)
L, t	height and thickness of the board, respectively (m)
L_h	height of each of the discrete heat sources (m)
M, N	number of grids in horizontal and vertical directions, respectively
N_1	number of grids up to the trailing edge of the board
N_2	total number of grids up to the end of the first heat source
N_3	total number of grids up to the start of the second heat source
N_4	total number of grids up to the end of the second heat source
N_5	total number of grids up to the start of the third heat source
N_{RF}	radiation–flow interaction parameter, $\sigma T_\infty^4/[k_f\Delta T_{ref}/L]$
P	pressure at any location in the computational domain (Pa)
Pe_L	Peclet number, $Re_L Pr$
Pr	Prandtl number of air
q_v	volumetric heat generation in each of the discrete heat source (W/m^3)
Re_L	Reynolds number, $u_\infty L/\nu_f$
Ri_L^*	modified Richardson number, $g\beta\Delta T_{ref}L/u_\infty^2$ or Gr_L^*/Re_L^2
T	temperature at any location in the computational domain (K or °C)
T_{max}	maximum temperature in the board (K or °C)

S. M. Sawant · C. Gururaja Rao (✉)
Department of Mechanical Engineering,
National Institute of Technology, Warangal 506 004,
Andhra Pradesh, India
e-mail: cgr_gcr@yahoo.co.in

T_∞ free stream temperature of air (K or °C)
u, v vertical and horizontal components of velocity of air (m/s)
u_∞ velocity of air (m/s)
U non-dimensional vertical velocity components of air, u/u_∞ or $\partial\psi/\partial Y$
V non-dimensional horizontal velocity components of air, v/u_∞ or $-\partial\psi/\partial X$
W width of the computational domain (m)
x vertical distance (m)
X non-dimensional vertical distance, x/L
y horizontal distance (m)
Y non-dimensional horizontal distance, y/L

Greek symbols

α thermal diffusivity of air (m^2/s)
β isobaric cubic expansivity of air, $-\frac{1}{\rho}\left(\frac{\partial\rho}{\partial T}\right)_p$ (K^{-1})
γ thermal conductance parameter, $k_f L/k_s t$
δ_c convergence criterion, in percentage, $|(\xi_{new}-\xi_{old})/\xi_{new}|\times 100\%$
ΔT_{ref} modified reference temperature difference, $q_v L_h t/k_s$ (K or °C)
Δx_f height of the board element chosen for energy balance in non-heat source portion (m)
Δx_h height of the board element chosen for energy balance in the heat source portion (m)
ε surface emissivity
θ non-dimensional temperature, $(T-T_\infty)/\Delta T_{ref}$
θ_{max} non-dimensional maximum board temperature
ν_f kinematic viscosity (m^2/s)
ξ any dependent variable (ψ, ω or θ) over which convergence is being tested for
ρ, ρ_∞ local and characteristic values of fluid density, respectively (kg/m^3)
σ Stefan–Boltzmann constant (5.6697×10^{-8} W/m^2 K^4)
ψ non-dimensional stream function, $\psi'/u_\infty L$
ψ' stream function (m^2/s)
ω non-dimensional vorticity, $\omega' L/u_\infty$
ω' vorticity (s^{-1})

Subscripts

cond, x, in conduction heat transfer into an element along the board
cond, x, out conduction heat transfer out of an element along the board
conv convection heat transfer from an element
new, old values of any variable from the current and previous iterations, respectively
rad heat transfer by surface radiation from an element

1 Introduction

A vertical plate is a commonly encountered geometry in the analyses pertaining to thermal control of electronic equipment. It very closely simulates the cooling passages of a series of printed circuit boards (PCBs) with heat generating components. The use of a known symmetric or asymmetric isothermal or isoflux boundary representation, which is being done in most of the analyses, only helps in the first-cut evaluation of the thermal performance of any given application. A more pragmatic analysis, however, is one, where the plate surface temperature distribution is not known a priori but must be determined as a part of the solution to the particular problem. A typical real life multi-mode heat transfer problem has internal conduction in the plate, followed by convection (both free and forced) and radiation from the plate surface.

Quite a large number of analytical, numerical and also experimental studies on free, forced or combined free and forced convection based on vertical plate geometry are available in the literature. Here, one can quote the references starting from [1], who provided the exact solution for fluid flow for the problem of laminar forced convection from an isothermal flat plate, way back in the year 1908. Several studies followed subsequently. The work on mixed convection started probably with [2], who studied, numerically, the effects of buoyancy on forced convection flow and heat transfer from a vertical flat plate. The works of [3–9] followed the queue.

However, the studies involving multi-mode heat transfer from the plate geometry are comparatively scarce. Among the earliest works reported on multi-mode heat transfer for the vertical plate geometry is the work of [10]. He investigated steady laminar natural convection heat transfer from a vertical heat-conducting flat plate of finite thickness with an arbitrary heating distribution on its surface. Following him are [11–16]. In the References 15 and 16 above, the authors considered a vertical plate with a single flush-mounted discrete heat source and studied, in detail, the interaction of surface radiation with mixed convection and conduction. However, a more realistic simulation to an electronic board would be a vertical plate with multiple heat sources.

In view of the above, in the present article, the problem of conjugate mixed convection with surface radiation from

a vertical plate with three identical flush-mounted discrete heat sources is investigated.

2 Mathematical formulation

Figure 1 shows the schematic of the problem geometry considered for study. It comprises a vertical electronic board simulated as a plate of height L and thickness t. The plate possesses three identical discrete heat sources, each of height L_h and volumetric heat generation q_v. The heat sources are flush-mounted in the plate, as shown. The plate is adiabatic on its left, top and bottom surfaces. Thus, the heat generated in the heat sources is first conducted along the board and is subsequently dissipated by mixed (combined free and forced) convection and radiation from the right surface of the plate into air, which is taken as the cooling medium.

The governing equations for fluid flow and heat transfer concerning the present problem are the continuity equation, Navier–Stokes equations and equation of energy, respectively, given as

$$\frac{\partial u}{\partial x}+\frac{\partial v}{\partial y}=0 \tag{1}$$

$$u\frac{\partial u}{\partial x}+v\frac{\partial u}{\partial y}=-\frac{1}{\rho}\frac{\partial P}{\partial x}+\nu\left(\frac{\partial^2 u}{\partial x^2}+\frac{\partial^2 u}{\partial y^2}\right)+g\frac{\rho_\infty}{\rho}-g \tag{2}$$

$$u\frac{\partial v}{\partial x}+v\frac{\partial v}{\partial y}=-\frac{1}{\rho}\frac{\partial P}{\partial y}+\nu\left(\frac{\partial^2 v}{\partial x^2}+\frac{\partial^2 v}{\partial y^2}\right) \tag{3}$$

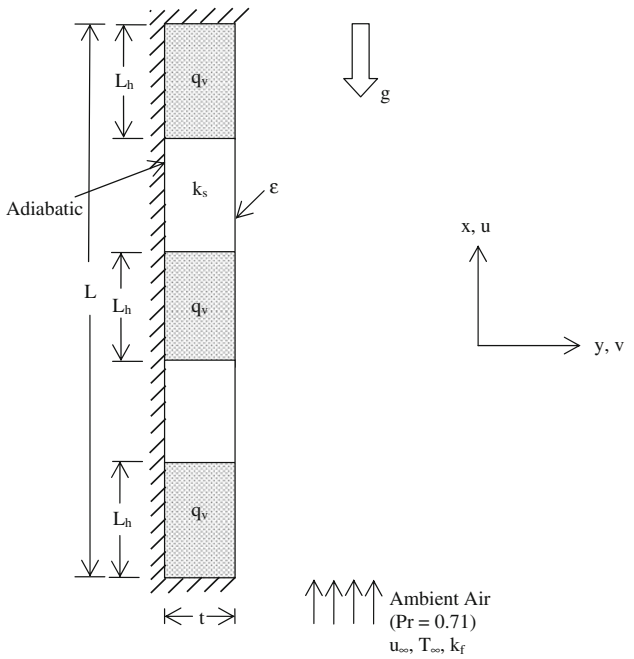

Fig. 1 Schematic of the problem geometry considered for study along with system of co-ordinates

$$u\frac{\partial T}{\partial x}+v\frac{\partial T}{\partial y}=\alpha\left(\frac{\partial^2 T}{\partial x^2}+\frac{\partial^2 T}{\partial y^2}\right) \tag{4}$$

The above equations in primitive variables are first converted into stream function-vorticity form using the definitions of stream function (ψ') and vorticity (ω'). The resulting equations are non-dimensionalised using appropriate normalising parameters [refer to List of symbols and Greek symbols elsewhere]. The normalised equations turn out to be

$$U\frac{\partial \omega}{\partial X}+V\frac{\partial \omega}{\partial Y}=-Ri_L^*\frac{\partial \theta}{\partial Y}+\frac{1}{Re_L}\left(\frac{\partial^2 \omega}{\partial X^2}+\frac{\partial^2 \omega}{\partial Y^2}\right) \tag{5}$$

$$\frac{\partial^2 \psi}{\partial X^2}+\frac{\partial^2 \psi}{\partial Y^2}=-\omega \tag{6}$$

$$U\frac{\partial \theta}{\partial X}+V\frac{\partial \theta}{\partial Y}=\frac{1}{Pe_L}\left(\frac{\partial^2 \theta}{\partial X^2}+\frac{\partial^2 \theta}{\partial Y^2}\right) \tag{7}$$

Here, Ri_L^* is the modified Richardson number, which delineates mixed convection into different regimes. A larger value of Ri_L^* implies asymptotic free convection limit, while a smaller value of Ri_L^* means asymptotic forced convection limit. The value $Ri_L^*=1$ implies pure mixed convection where typically buoyancy and inertia forces are comparable. The Eqs. (5)–(7) are to be now solved in conjunction with the boundary conditions shown in Fig. 2. The figure shows use of extended computational domain in the present solution. This is done to capture the fluid flow and heat transfer more fully. It can be seen that the total height of computational domain is $2L$ and the width (W) of the domain is L. It is also to be noted that the present problem is being solved by considering the governing equations without boundary layer approximations (see [15]). With regard to the plate, the temperature varies axially [$T(x)$] owing to multi-mode heat transfer [heat generation accompanied by internal conduction followed by mixed convection and radiation from the surface]. In this context, the governing equations for temperature distribution along the plate are obtained by appropriate energy balance. The plate here, as can be seen from Fig. 1, has different portions, namely bottom and top adiabatic ends, heat source portions, non-heat source portions and interfaces between heat sources and the rest of the plate. For example, the energy balance on the element within one of the three heat sources yields:

$$q_{\mathrm{cond},x,\mathrm{in}}+q_v(\Delta x)t=q_{\mathrm{cond},x,\mathrm{out}}+q_{\mathrm{conv}}+q_{\mathrm{rad}} \tag{8}$$

Substitution of various terms in the above equation and subsequent simplification results in:

$$k_s t\frac{\partial^2 T}{\partial x^2}+k_f\left(\frac{\partial T}{\partial y}\right)_{y=0}+q_v t-\sigma\varepsilon\left(T^4-T_\infty^4\right)=0 \tag{9}$$

The above equation after non-dimensionalisation gives the required governing equation for non-dimensional

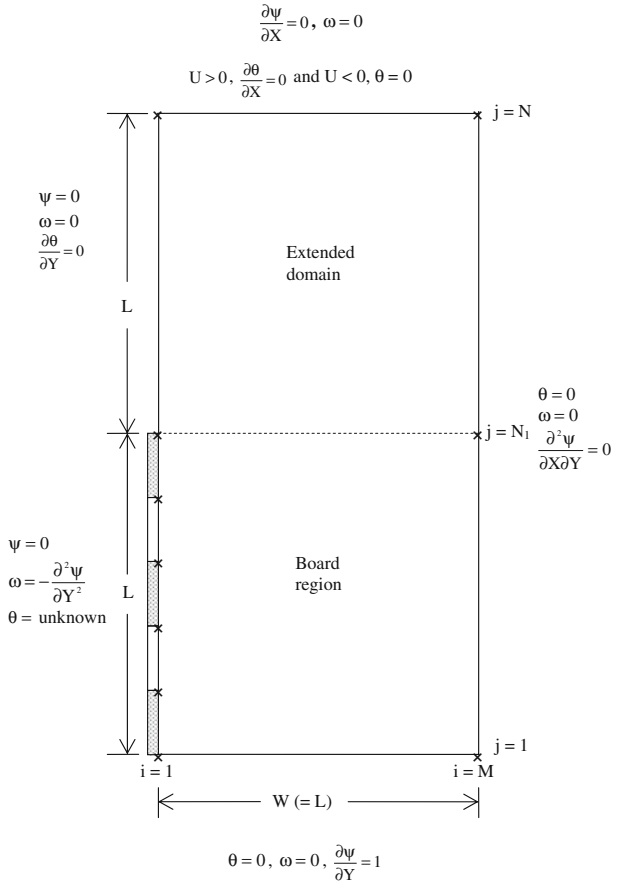

Fig. 2 Computational domain pertaining to the problem along with boundary conditions

temperature distribution for the elements within the heat sources as:

$$\frac{\partial^2\theta}{\partial X^2}+\gamma\left(\frac{\partial\theta}{\partial Y}\right)_{Y=0}+A_{r1}A_{r2}-\varepsilon\gamma N_{\mathrm{RF}}\left[\left(\frac{T}{T_\infty}\right)^4-1\right]=0 \tag{10}$$

The governing equations pertaining to the rest of the plate are also obtained in a similar manner.

3 Method of solution

The Eqs. (5)–(7) are non-linear elliptic partial differential equations. They are first converted into algebraic form using the finite volume based finite difference method of [17]. The resulting equations are then solved using Gauss–Seidel iterative technique. Under relaxation with a relaxation parameter of 0.5 is used on stream function and vorticity, while for temperature full relaxation is used. To terminate the iterations, strict convergence criteria of 1×10^{-4}, 5×10^{-4} and 1×10^{-4} are imposed on stream function, vorticity and temperature, respectively. A computer code in C is specifically written to solve the present problem.

4 Range of parameters

Calculations are made assuming the height (L) and the thickness (t) of the electronic board to be, respectively, equal to 20 cm and 1.5 mm, respectively. The height (L_h) of each discrete heat source is taken to be $L/8$ (or 2.5 cm), while the thickness of the heat source would be the same as that of the board itself (i.e., 1.5 mm). The cooling agent, air, is assumed to be of constant thermo physical properties, with the value of Prandtl number (Pr) taken to be 0.71. The free stream temperature (T_∞) of air is taken to be 25°C. The surface emissivity (ε) of the board is varied between 0 and 1, implying minimum and maximum radiation limits. However, since typically 0.05 and 0.85 are surface emissivities pertaining to poor emitter (good reflector) and good emitter (poor reflector), respectively, most of the studies in the present work too have considered the above limiting values for surface emissivity. With regard to modified Richardson number Ri^*_L, a range of 25–0.1 is chosen. Here, $Ri^*_L = 25$ and 0.1 signify, respectively, the asymptotic limits of free and forced convection, while $Ri^*_L = 1$ indicates pure mixed convection regime. The thermal conductivity (k_s) of the board is varied between 0.25 and 1. This is done keeping in mind that typically electronic boards are made of a material with thermal conductivity of the order of unity [for example, Mylar coated epoxy glass generally used in this kind of applications has thermal conductivity equal to 0.26 W/m K]. The volumetric heat generation (q_v) in each of the heat sources is also a variable, though in the present paper, all the results that are shown are for $q_v = 10^6$ W/m^3.

5 Results and discussion

5.1 Grid convergence test

In order to freeze on the optimum grid system for discretisation of the computational domain [dimensions $2L \times L$], a detailed grid sensitivity analysis is taken up. Figure 3 shows a notional representation of the discretised computational domain, wherein finer uniform grids are chosen along the three heat sources. Coarser uniform grids are considered along the two non-heat source portions of the board and the extended length of the computational domain in the vertical direction. Here again the grids in the extended length are coarser. In the horizontal direction, since the velocity and temperature gradients near the

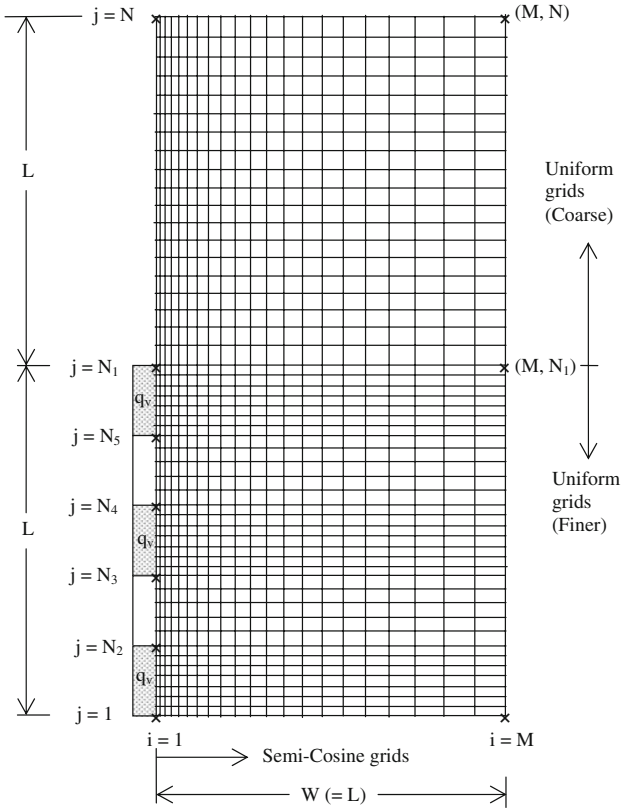

Fig. 3 Grid system used for discretisation of the computational domain

surface of the board are steeper than those away from the board, a semi-cosine grid system is used.

The grid convergence test is performed in four stages. In each stage, the study is conducted for three typical values of Ri_L^*, viz., 25, 1 and 0.1. In the present paper, however, the results are shown only for $Ri_L^* = 1$ as can be seen from Tables 1, 2, 3, 4. In stage 1 (Table 1), the total number of grids in the vertical direction (N) is arbitrarily taken to be 151, while 20 grids are chosen in each heat source, with the number of grids up to the trailing edge of the board (N_1) taken to be 101. The number of grids in the horizontal direction (M) is varied here. It can be seen that there is a progressive convergence in the value of θ_{max} (peak non-dimensional board temperature) as the value of M increases from 81 in steps of 10. Since the change in θ_{max} from $M = 111$ to 121 is only by 0.14%, the value of M is fixed to be 111 for the entire work in the present paper. In stage 2 (Table 2), M is fixed at the value frozen in stage 1 (111). The number of grids in each heat source is taken to be 20 and N_1 is taken equal to 101. The total number of grids along the vertical direction (N) is varied here. The table indicates a change of 0.003% in θ_{max} as N changes from 141 to 151, while, the change in θ_{max} raises to 0.004% for a further increase of N from 151 to 161. In view of this, N is fixed to be 151 for the entire study. Stage 3 of the study considers the frozen values of $M = 111$ and $N = 151$. The number of grids in each heat source is taken equal to 20 and the number of grids along the board (N_1) is varied. Table 3 shows that there is a change in θ_{max} by 0.009% as N_1 increases from 101 to 111. A further increase in N_1 to 121 changes θ_{max} by 0.03%. Owing to this, N_1 is fixed to be 111 for the entire study. Finally, keeping $M = 111$, $N = 151$ and $N_1 = 111$ fixed (frozen from stages 1 to 3), the number of grids along each heat source is varied in stage 4. Table 4 shows the above results. It can be seen that θ_{max} changes only by 0.148% as the number of grids along each heat source is varied from 24 to 30. Thus 24 grids are fixed along each heat source for entire study. To summarise, the grid convergence test has resulted in an optimum

Table 1 First stage of grid convergence test

S. No.	M	θ_{max}	Percentage change (abs.)
1	81	0.5149392	–
2	91	0.5164226	0.2880728
3	101	0.5174605	0.2009788
4	111	0.5183474	0.1713947
5	121	0.5190790	0.1411409
6	131	0.5194383	0.0692187

[$k_s = 0.25$ W/m K, $\varepsilon = 0.45$, $q_v = 10^6$ W/m^3, $Ri_L^* = 1$] $N = 151$, $N_1 = 101$, $N_2 = 21$, $N_3 = 41$, $N_4 = 61$ and $N_5 = 81$

Table 2 Second stage of grid convergence test

S. No.	N	θ_{max}	Percentage change (abs.)
1	131	0.5183801	–
2	141	0.5183327	0.0091439
3	151	0.5183474	0.0028360
4	161	0.5183286	0.0036269
5	171	0.5184255	0.0186947
6	181	0.5184693	0.0084487

[$k_s = 0.25$ W/m K, $\varepsilon = 0.45$, $q_v = 10^6$ W/m^3, $Ri_L^* = 1$] $M = 111$, $N_1 = 101$, $N_2 = 21$, $N_3 = 41$, $N_4 = 61$ and $N_5 = 81$

Table 3 Third stage of grid convergence test

S. No.	N_1	θ_{max}	Percentage change (abs.)
1	81	0.5183073	–
2	91	0.5184220	0.0221297
3	101	0.5183474	0.0143898
4	111	0.5183934	0.0088744
5	121	0.5185422	0.0287041
6	131	0.5186824	0.0270373

[$k_s = 0.25$ W/m K, $\varepsilon = 0.45$, $q_v = 10^6$ W/m^3, $Ri_L^* = 1$] $M = 111$, $N = 151$ and number of grids per heat source = 20

Table 4 Fourth stage of grid convergence test

S. No.	Number of grids in each heat source	θ_{max}	Percentage change (abs.)
1	6	0.5096876	–
2	12	0.5158541	1.2098587
3	18	0.5179040	0.3973798
4	24	0.5189700	0.2058297
5	30	0.5197392	0.1482167

[$k_s = 0.25$ W/m K, $\varepsilon = 0.45$, $q_v = 10^6$ W/m^3, $Ri_L^* = 1$] $M = 111$, $N = 151$, $N_1 = 111$

grid system with $M = 111$, $N = 151$, $N_1 = 111$, $N_2 = 25$, $N_3 = 44$, $N_4 = 68$ and $N_5 = 87$.

5.2 Check for energy balance

After the identification of the optimum grid system, results are obtained for some typical cases to check the code developed in the present study for the energy balance. To do so, the net rate of heat dissipation from the board by the cumulative effect of mixed convection and radiation is obtained by integrating the local convective and radiative heat fluxes over the entire area of the board. The above calculation is compared with the net rate of heat generation in the board. The check is made in the entire regime of convection ($Ri_L^* = 0.1$–25) for varying values of other input parameters [k_s, ε and q_v]. It has been noticed that the energy balance works out quite satisfactorily within the maximum deviations of ± 0.008, 0.09 and 0.26%, respectively, for the values of $Ri_L^* = 0.1$, 1 and 25. Similar trends have been noticed for other values of Ri_L^* as well. This serves to check the mathematical accuracy of the present problem.

5.3 Validation

The results of the present problem are validated for the asymptotic limiting case of mixed convection from an isothermal vertical flat plate. Here, again, the comparison is made in forced convection dominant, pure mixed convection and free convection dominant regimes. A good parity has been noticed between the results of the present problem and (1) Blasius [1] in asymptotic forced convection limit, (2) Gururaja Rao et al. [9] in pure mixed convection and (3) Ostrach [18] in asymptotic free convection limit, with deviations limited to a maximum of about $\pm 1.01\%$. Thus, there exists a good validation for the results of the present problem.

5.4 Local temperature distribution along the board

One of the prime points of interest in the present study is the effect of various parameters on the nature of variation of temperature along the board.

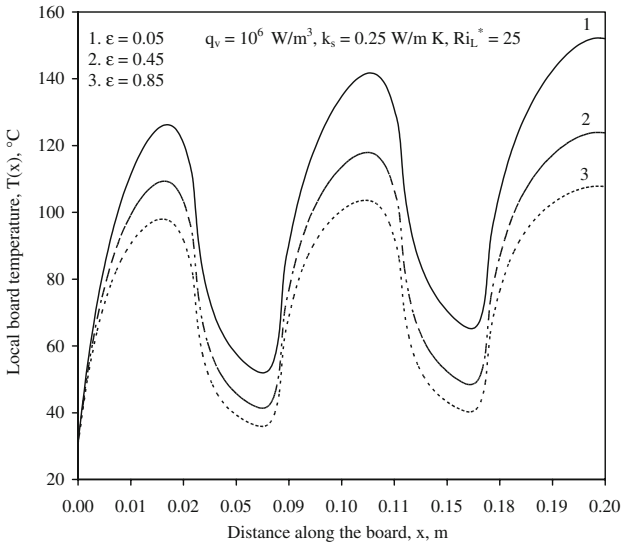

Fig. 4 Variation of local board temperature with surface emissivity

Figure 4 shows the local board temperature profiles for three values of surface emissivity, viz., $\varepsilon = 0.05$, 0.45 and 0.85. The results are obtained for $q_v = 10^6$ W/m^3, $k_s = 0.25$ W/m K and $Ri_L^* = 25$. It can be seen that all the three local temperature profiles exhibit a similar pattern. For a given surface emissivity, the local temperature is increasing sharply to some maximum value somewhere near the end of the first heat source and is again dropping down sharply as one goes through the non-heat source portion between first and second heat sources. After reaching a local minimum, the temperature again increases and a similar behaviour as noticed along the first heat source is observed along the second heat source portion as well. However, with regard to the third heat source, the temperature reaches the peak just near the trailing edge of the board. The above peak temperature is incidentally the maximum of the three local peaks and thus is the maximum temperature along the board. The observation of the three local peaks in the three heat source portions of the board is due to the occurrence of bulk of heat transfer activity in those regions. Further, the reason for the progressive increase of peak temperature as one moves from the leading to the trailing edge of the board may be attributed to the progressive decrease in the rate of local heat dissipation by convection and radiation. The reason for this, in turn, is the continuous reduction in the local temperature difference between the board and the fluid in the above direction. The figure also reveals that, at any given location along the board, the temperature decreases with increasing surface emissivity of the board. For example, in the case considered here, the first local peak, the second local peak and the maximum board temperature are decreasing, respectively, by 13.35, 16.80 and 18.57% as ε increases from 0.05 to 0.45. The above temperatures further

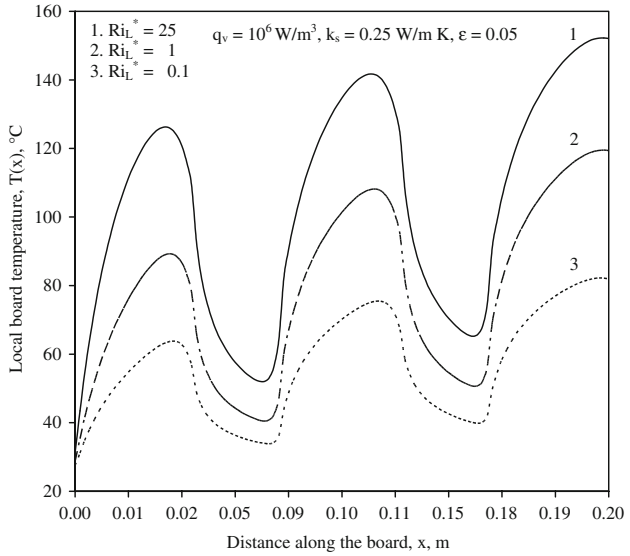

Fig. 5 Variation of local board temperature in different regimes of mixed convection

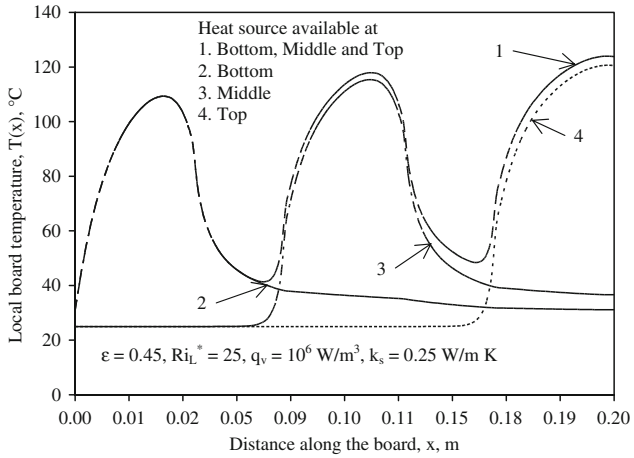

Fig. 6 Local board temperature profiles for varying positions and combinations of heat sources

decrease, respectively, by 10.40, 12.11 and 13.01% as ε subsequently increases to 0.85. Thus, in total, there is a drop of 29.17% in T_{max} as ε increases from 0.05 to 0.85.

Figure 5 shows local board temperature profiles plotted in three different regimes of convection, namely $Ri_L^* = 25$, 1 and 0.1. The above figure pertains to the case with $q_v = 10^6$ W/m^3, $k_s = 0.25$ W/m K and $\varepsilon = 0.05$. The local board temperature for a given value of Ri_L^* appears to be following the trend similar to that followed in Fig. 4. Like in the case of Fig. 4, there are three local peaks and two local minima for each curve, with the third local peak being the maximum board temperature. The figure reveals that, for a given thermal conductivity of the board (k_s) and surface emissivity (ε), the temperature at any location along the board decreases as one moves from free convection dominant regime to forced convection dominant regime. This is in view of the increased convection activity from the surface of the board owing to increased free stream velocity of the cooling medium (air). For example, the first, the second and the third local peak temperatures along the board decrease by 49.45, 46.78 and 45.99% as Ri_L^* changes from 25 to 0.1. The figure, thus, explains the role of impressed velocity (u_∞) in influencing the board temperature for the given values of material and surface properties (k_s and ε).

It would be interesting to study the variation of local board temperature by having one of the three heat sources at a time and comparing the variation with that in the conventional case in which all the three heat sources are present. Figure 6 shows exactly this for the case where $q_v = 10^6$ W/m^3, $Ri_L^* = 25$, $k_s = 0.25$ W/m K and $\varepsilon = 0.45$. The curves 1, 2, 3 and 4 pertain to the cases, namely (1) all the three heat sources present (2) the heat source at the leading edge alone present (3) the central heat source alone present and (4) the heat source at the trailing edge alone present. The local temperature profile pertaining to case 1 is like what has been noticed in Figs. 4 and 5 above. With regard to the case 2, where the heat source at the leading edge alone is present, major heat transfer activity could be noticed in the initial 7.5 cm length of the board, while in the remaining portion of 12.5 cm, the temperature gradient along the board diminishes considerably. This is because of the fact that the above portion of the board does not possess any further heat source in it but merely conducts the heat that is generated in the only heat source that is located at the leading edge. Likewise in the case 3, where only the central heat source is present, the major activity of heat transfer is in the central portion of the board spread over a length of about 10 cm. In the last case, where the heat source is only at the trailing edge of the board, the last 5 cm length of the board towards the trailing edge plays active role in heat conduction, while the remaining portion of the board hardly shows any activity. The reason for the above nature of variation with regard to cases 3 and 4 is the same as narrated above with regard to case 2. Further, the figure also indicates that there is a progressive increase in T_{max} from case 2 to case 4. This means that the trailing edge of the board is the least preferable position for the heat source, if one were required to use a single heat source along the entire board. The above observation coincides with the findings of [9, 15]. This serves as substantiation of the validity of the results of the present code. It is further clear from the present figure that the value of T_{max} with all the three heat sources present is greater than any of the peaks noticed in cases 2, 3 and 4. This is justified on account of threefold increment in q_v when all the three heat sources are present.

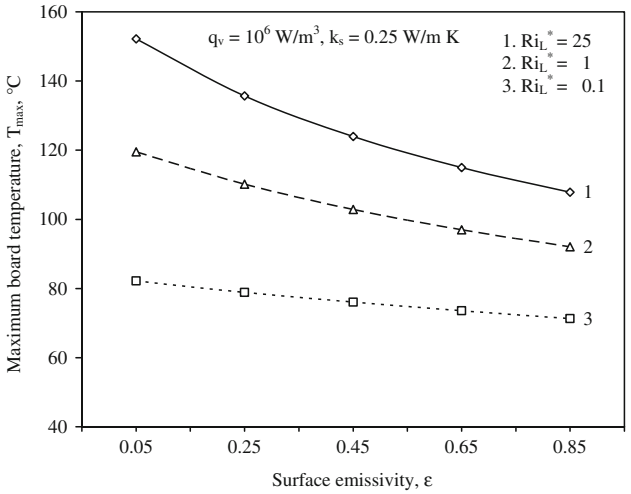

Fig. 7 Variation of maximum board temperature with surface emissivity in different regimes of mixed convection

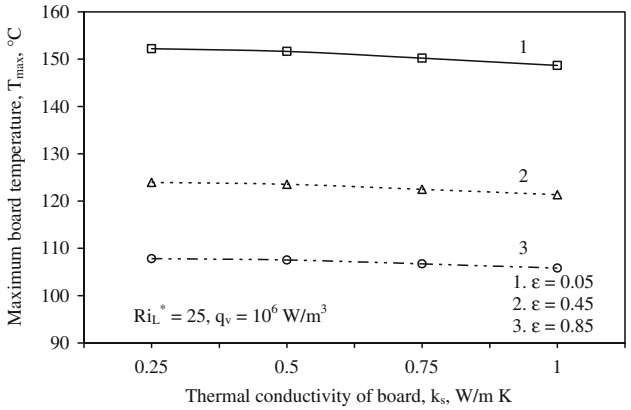

Fig. 8 Variation of maximum board temperature with thermal conductivity of board material for different surface emissivities

5.5 Variation of maximum board temperature with other parameters

The variation of the maximum board temperature with surface emissivity in different regimes of mixed convection is shown in Fig. 7. The results are obtained for $q_v = 10^6$ W/m^3 and $k_s = 0.25$ W/m K. The three regimes of mixed convection chosen are (1) free convection dominant regime ($Ri_L^* = 25$), (2) pure mixed convection regime ($Ri_L^* = 1$) and (3) forced convection dominant regime ($Ri_L^* = 0.1$). Five of the possible surface coatings of the board with emissivity (ε) equal to 0.05, 0.25, 0.45, 0.65 and 0.85 are considered for study. The figure reveals that, even though T_{max} generally decreases with increasing ε, the influence of ε is more pronounced in free convection dominant regime and less pronounced in forced convection dominant regime, with the pure mixed convection regime exhibiting a behaviour somewhere in between. For example, in the case considered here, the peak board temperature comes down by 29.17% as ε increases from 0.05 to 0.85 for $Ri_L^* = 25$. For $Ri_L^* = 1$ and 0.1, the decrease in T_{max} between the same limits of ε (0.05 and 0.85) is found to be 22.97 and 13.25%, respectively. This study demonstrates the relevance of surface coating in influencing peak board temperature in all regimes of convection, specifically in the cases of free convection.

A family of curves depicting the nature of variation of peak board temperature (T_{max}) with thermal conductivity of the material of the board (k_s) is shown in Fig. 8. The curves are plotted covering three typical values of ε, namely 0.05, 0.45 and 0.85, for the case of free convection dominant regime ($Ri_L^* = 25$). It can be seen that, for a given surface emissivity, there is only a minimal decrease in T_{max} with increasing k_s. This is because of smaller values of thermal conductivity employed in the present study, which results in a non-significant variation in the heat transfer activity along the board when all the remaining parameters governing the problem are held fixed. However, for a given thermal conductivity, the figure shows a considerable drop in T_{max} with increase in surface emissivity. This result substantiates the dominant role of surface radiation, when one works in the free convection regime. For example, in the present case, for $k_s = 0.5$ W/m K, T_{max} comes down by 18.54% as ε rises from 0.05 to 0.45 and by a further 12.94% as ε subsequently rises to 0.85. The above trends have been noticed even in other regimes of convection also.

5.6 Exclusive effect of surface radiation on the results of the problem

In order to bring out exclusively the effect surface radiation has on the present problem, results are obtained for local board temperature distribution and peak board temperature with ε equal to 0 and 1. The above two values, respectively, indicate the cases without radiation and with maximum possible radiation. Figure 9 is drawn based on the results for the case with $q_v = 10^6$ W/m^3, $k_s = 0.25$ W/m K and $Ri_L^* = 25$. The figure clearly shows that, at any given location along the board, there is a marked drop in the temperature when once radiation is reckoned with. This is the case with almost the entire length of board but for some initial portion at the leading edge where the fluid flow is just commencing. In the present example, the first, the second and the third local peak temperatures along the board for the case where no radiation is considered are, respectively, 129.01, 146.03 and 157.58°C. When once the electronic board is assumed to be dissipating heat by radiation with its surface coated with, say, lamp black soot ($\varepsilon = 1$), the above three temperatures are coming down to 94.55, 99.51 and 103.26°C. Thus, there is an error of the

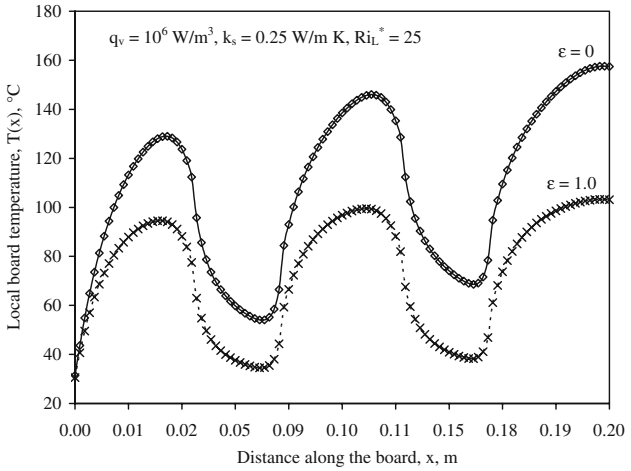

Fig. 9 Local board temperature profiles in a given regime of convection showing exclusive effect of surface radiation

order of 34.47% in the local temperature calculation along the board if one ignores radiation in the present problem.

Figure 9 discussed above pertains to exclusive effect of radiation on local temperature in a particular regime of convection ($Ri_L^* = 25$). In order to study as to what kind of an effect surface radiation exclusively shows on the results of the present problem in various regimes of convection, Fig. 10 is plotted. It shows maximum board temperature drawn against modified Richardson number in the two extreme cases of no radiation ($\varepsilon = 0$) and maximum possible radiation ($\varepsilon = 1$). The study pertains to the case with constant values of q_v and k_s as shown in the figure. As many as seven values of Ri_L^* are chosen covering the whole range of mixed convection regime ($Ri_L^* = 0.1$–25). It can be seen that, in all the regimes of convection, there is a significant effect of surface radiation in controlling the peak board temperature. The above effect is to a lesser degree for $Ri_L^* = 0.1$ and gradually increases towards larger values of Ri_L^*, with maximum effect seen at $Ri_L^* = 25$. In the present example, when compared to the case that ignores radiation, radiation with $\varepsilon = 1$ is bringing down T_{max} by 16.02, 27.31 and 34.47% for $Ri_L^* = 0.1$, 1 and 25.

5.7 Roles played by mixed convection and radiation in heat dissipation from the board

As already mentioned in the problem definition, the dissipation of heat from the board is shared by mixed convection and radiation. In view of this, a study is made to delineate the contributions from mixed convection and radiation in various regimes of convection. Figure 11 shows this for the case with $q_v = 10^6$ W/m^3 and $k_s = 0.25$ W/m K. Five typical values of surface emissivity are chosen, namely $\varepsilon = 0.05$, 0.25, 0.45, 0.65 and 0.85, and three different regimes of convection ($Ri_L^* = 25$, 1 and 0.1) are selected. The figure indicates that in a given regime of convection, the contribution to heat dissipation by convection progressively decreases as ε rises from 0.05 to 0.85, with the contribution from radiation showing a mirror image increase. However, for $Ri_L^* = 0.1$, indicating forced convection dominant regime, there is an expected dominance from convection, with radiation showing a limited role. In the present example, for $Ri_L^* = 0.1$, the contribution from convection is ranging between 98.40 and 78.88% as ε changes from 0.05 to 0.85. In contrast, here, radiation is contributing a maximum of 21.12% for the upper limit of emissivity (0.85) chosen. As one moves towards pure mixed convection regime ($Ri_L^* = 1$), radiation starts playing an enhanced role, with its contribution to heat dissipation increasing from 3.03 to 32.94% as ε varies

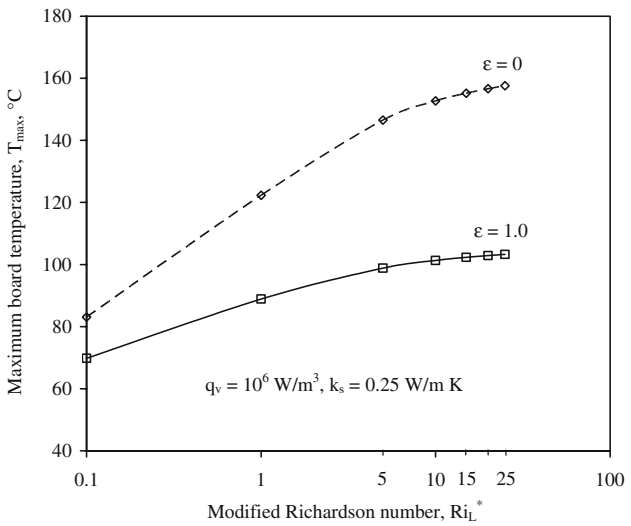

Fig. 10 Peak board temperature in various regimes of convection demonstrating exclusive effect of surface radiation

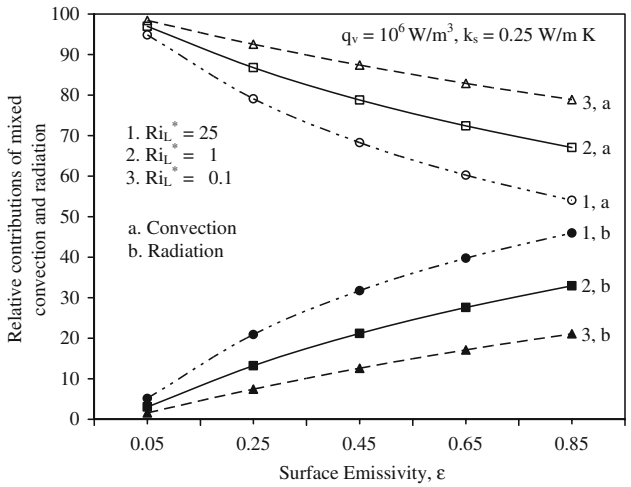

Fig. 11 Relative contributions of mixed convection and radiation with surface emissivity in different regimes of mixed convection

from 0.05 to 0.85. In the asymptotic free convection limit ($Ri_L^* = 25$), radiation is at its best, with as much as 45.94% contributed by it for the value of $\varepsilon = 0.85$. The above study elucidates the importance of radiation in the present problem in different regimes of convection and any calculation without its consideration is bound to be error prone.

5.8 Exclusive role played by buoyancy in mixed convection

Since in the present problem, the convection heat transfer is due to the combined effects of buoyancy and inertia forces, efforts are made to bring out the exclusive effect of buoyancy on both local temperature distribution and peak board temperature. Figures 12 and 13 narrate the results of the above.

Figure 12 explains the variation of local board temperature for the cases with (1) forced convection alone and (2) buoyancy aiding forced convection, i.e., mixed convection, for a given value of surface emissivity ($\varepsilon = 0.05$). It can be seen that there is a continuous decrement in the temperature along the board when once buoyancy is reckoned with. However, the degree of decrement in the local board temperature is more pronounced in the regions where there are heat sources than those without the heat sources. Further, of all the three heat sources, buoyancy exhibits more dominance near the trailing edge of the board, where the third heat source is present. This is expected because the denser air near the trailing edge of the board gets down the board, picks up the heat from the surface of the board, gets lighter, and thus again rises up along the board. Therefore, the buoyancy effect will obviously be the maximum near the trailing edge of the board and gets progressively

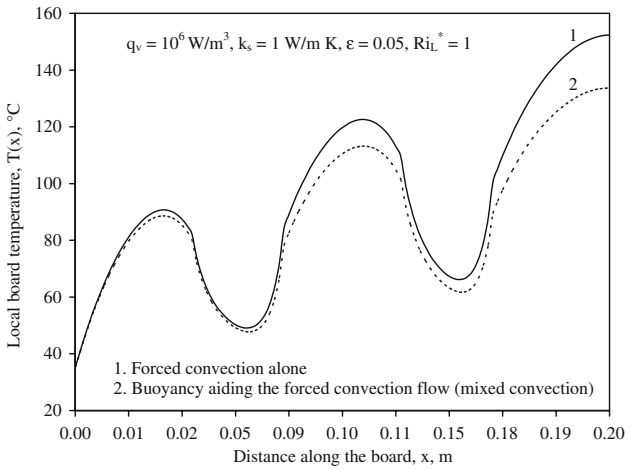

Fig. 12 Local board temperature profiles in a given regime of mixed convection showing the exclusive effect of buoyancy

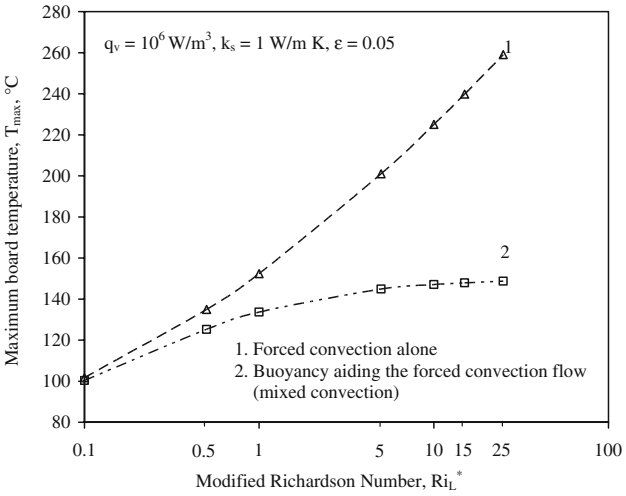

Fig. 13 Variation of maximum board temperature in different regimes of mixed convection highlighting the exclusive effect of buoyancy

diminished as one moves down towards the leading edge. In the present example, the local peak temperatures in the first, second and third heat sources counted from the leading edge of the board are 90.71, 122.56 and 152.33°C when forced convection alone is considered. The above temperatures are getting reduced, respectively, to 88.58, 113.19 and 133.67°C when once buoyancy effect is accounted for.

The variation of maximum board temperature with modified Richardson number for the given values of ε (0.05) and k_s (1 W/m K) is shown in Fig. 13. Curves 1 and 2, respectively, indicate the cases where (1) only forced convection is considered and (2) buoyancy that assists forced convection is also considered. As many as seven values of Ri_L^* are chosen for study encompassing the entire regime of convection ($0.1 \leq Ri_L^* \leq 25$). It can be seen that, for smaller values of Ri_L^* (0.1–1.0), though there is a drop in the peak board temperature due to the consideration of buoyancy in addition to inertia forces, the impact is not very significant. However, towards larger values of Ri_L^*, the role of buoyancy in bringing down the maximum board temperature is assuming greater importance. The above is attributed to the fact that, for larger values of Ri_L^*, the order of magnitude of inertia forces is far less than that of buoyancy forces. Thus, any attempt to undermine buoyancy (free convection component) here would over estimate the peak temperature attained by the board. This results in incorrect design of cooling system for a given electronic device. For example, in the case discussed here, the peak board temperature is overestimated by 1.36, 13.96 and 74.21% when a designer ignores buoyancy in comparison to forced convection for the values of Ri_L^* equal to 0.1, 1 and 25, respectively.

6 Concluding remarks

A numerical investigation into the problem of combined conduction-mixed convection-surface radiation from a vertical electronic board equipped with three identical flush-mounted discrete heat sources has been made. The governing equations that have been considered without boundary layer approximations are solved using the finite volume based finite difference method. A computer code is written specifically for the purpose. An extended computational domain has been employed and a 151×111 grid system is used to discretise the computational domain. The results, like local board temperature distribution, peak board temperature and relative contributions of mixed convection and surface radiation to heat transfer from the board have been studied by varying independent parameters, such as thermal conductivity, surface emissivity and modified Richardson number. Exclusive impact of surface radiation on the results of the present problem has been brought out. Results are obtained even to bring out the exclusive effect of buoyancy (free convection component) on the problem. The facts that one cannot ignore (1) buoyancy component in a convection environment and (2) surface radiation in a heat transfer application employing a gaseous cooling agent have been exhaustively demonstrated.

References

1. Blasius H (1908) Grenzschichten in Flussigkeiten mit kleiner Reibung. Z Math Phys 56:1, as reported in Chapman AJ Heat Transfer. Macmillan, New York, 1989
2. Sparrow EM, Gregg JL (1959) Buoyancy effects in forced convection flow and heat transfer. ASME J Appl Mech 81:133–134
3. Lloyd JR, Sparrow EM (1970) Combined forced and free convection flow on vertical surfaces. Int J Heat Mass Transfer 13:434–438
4. Wilks G (1973) Combined forced and free convection flow on vertical surfaces. Int J Heat Mass Transfer 16:1958–1964
5. Ramachandran N, Armaly BF, Chen TS (1985) Measurements and predictions of laminar mixed convection flow adjacent to a vertical surface. ASME J Heat Transfer 107:636–641
6. Chen TS, Armaly BF, Ramachandran N (1986) Correlations for laminar mixed convection flows on vertical, inclined and horizontal flat plates. ASME J Heat Transfer 108:835–840
7. Chen TS, Armaly BF, Aung W (1985) Mixed convection in laminar boundary-layer flow. In: Kakac S, Aung W, Viskanta R (eds) Natural convection: fundamentals and applications. Hemisphere, Washington, pp 699–725
8. Kishinami K, Saito H, Suzuki J, Ali AHH, Umeki H, Kitano N (1998) Fundamental study of combined free and forced convective heat transfer from a vertical plate followed by a backward step. Int J Numer Methods Heat Fluid Flow 8:717–736
9. Gururaja Rao C, Balaji C, Venkateshan SP (2000) Numerical study of laminar mixed convection from a vertical plate. Int J Transp Phenomena 2:143–157
10. Zinnes AE (1970) The coupling of conduction with laminar natural convection from a vertical flat plate with arbitrary surface heating. ASME J Heat Transfer 92:528–534
11. Tewari SS, Jaluria Y (1990) Mixed convection heat transfer from thermal sources mounted on horizontal and vertical surfaces. ASME J Heat Transfer 112:975–987
12. Hossain MA, Takhar HS (1996) Radiation effect on mixed convection along a vertical plate with uniform surface temperature. Heat Mass Transfer/Waerme Stoffuebertrag 31:243–248
13. Merkin JH, Pop I (1996) Conjugate free convection on a vertical surface. Int J Heat Mass Transfer 39:1527–1534
14. Cole KD (1997) Conjugate heat transfer from a small heated strip. Int J Heat Mass Transfer 40:2709–2719
15. Gururaja Rao C (2004) Buoyancy-aided mixed convection with conduction and surface radiation from a vertical electronic board with a traversable discrete heat source. Numer Heat Transfer Part A 45:935–956
16. Gururaja Rao C, Balaji C, Venkateshan SP (2001) Conjugate mixed convection with surface radiation from a vertical plate with a discrete heat source. ASME J Heat Transfer 123:698–702
17. Gosman AD, Pun WM, Runchal AK, Spalding DB, Wolfshtein M (1969) Heat and mass transfer in recirculating flows. Academic Press, New York
18. Ostrach S (1953) An analysis of laminar free convection flow and heat transfer about a flat plate parallel to the generating body force. NACA Rep.1111, as reported in Chapman AJ Heat Transfer. Macmillan, New York, 1989